Psychophysiology, 38 (2001), 607–621. Cambridge University Press. Printed in the USA.

Sequence-sensitive subcomponents of P300: Topographical analyses and dipole source localization

INES JENTZSCH AND WERNER SOMMER

Department of Psychology, Humboldt-University Berlin, Germany

Abstract

P300 amplitude and reaction time (RT) are strongly affected by the sequence of events preceding the eliciting stimulus. Sommer, Leuthold and Soetens (1999) found that robust sequential effects in P300 amplitude could be dissociated from more variable sequential effects in RTs. However, global changes in P300 amplitude and topography gave rise to the suggestion that sequential effects are specific for a subcomponent of P300 that is separate from and anterior to the classical parietal P300. Here, confirming evidence for dissociable subcomponents of P300 is reported from two experiments. Independent component analysis separated a centrally distributed sequence-sensitive subcomponent from a more parietal subcomponent. Subsequent dipole source analysis indicated a deep mesial source for the sequence-sensitive subcomponent. Overlap with reafferent somatosensory activity appears to be responsible for an apparent lateralization of this component towards the hemisphere ipsilateral to the responding hand.

Descriptors: P300, Movement-related potentials, Sequential effects, ICA, Source localization

In many experiments that use continuous presentation of several alternative stimuli, event-related brain potentials (ERPs) are not only influenced by the current stimulus but also by the sequence of preceding events. Sequential effects in ERPs were first reported by Squires, Wickens, Squires, and Donchin (1976). Relatively small amplitudes of the P300 and surrounding components in the ERP were observed after repeated presentations of the same stimulus (repetition runs) as well as for continued runs of stimulus alternations. Stimuli that discontinued such runs, that is, a stimulus alternation after several repetitions or a stimulus repetition after several alternations, elicited large ERP amplitudes.

The sequential effects in ERP amplitudes, reported by Squires et al. (1976) and subsequently confirmed by many others (e.g., Duncan-Johnson, Roth, & Kopell, 1984; Ford, Duncan-Johnson, Pfefferbaum, & Kopell, 1982; Sommer, Matt, & Leuthold, 1990), resembled the sequential effects that had previously been observed in reaction times (RTs). The sequential effects in RTs had been explained by confirmations and disconfirmations of expectancies that are presumably induced by the sequence of preceding stimuli (e.g. Bertelson, 1963; Hyman, 1953; Kirby, 1980). If expectancy is confirmed, RT is short and, if it is disconfirmed, RT is long. Because of the similarity of sequential effects in RTs and ERP amplitudes, Squires et al. generalized the expectancy concept also to the explanation of sequential effects in ERPs.

We thank Scott Makeig and his colleagues for the very valuable advice regarding the application of independent component analysis onto our data. We also thank Hartmut Leuthold for helpful discussions and comments on preliminary versions of this article.

Address reprint requests to: Ines Jentzsch, 58 Hillhead Street, Department of Psychology, University of Glasgow, Glasgow G12 8QB, United Kingdom. E-mail: ines@psy.gla.ac.uk.

In recent years, it has been shown that sequential effects in RTs are affected by a number of variables and may show properties that are not explainable by expectancy. The most systematic analysis of sequential effects and their antecedent conditions in RTs has been performed by Soetens and coworkers (Soetens, Boer, & Hueting, 1985; Soetens, Deboeck, & Hueting, 1984). Soetens introduced a nomenclature for describing sequential effects that will be adopted here as well. Each event is coded according to whether it constitutes a repetition (R) or an alternation (A) relative to its predecessor. Thus RRRA denotes a run of three stimulus repetitions, discontinued by an alternation as the last (current) stimulus. Furthermore Soetens distinguished between first-order and higher order sequences. First-order sequential effects are the consequences of the stimulus immediately preceding the current stimulus; that is, the current stimulus can be either a repetition or an alternation with respect to its predecessor. Higher order sequential effects are the consequences of the events further back in the sequence.

The main factors that influence sequential patterns in two-choice RT tasks are the interval between the response and the next stimulus (response stimulus interval, RSI) and stimulus response compatibility. In spatially compatible stimulus response assignments and for RSIs greater than about 500 ms, RTs systematically follow the common expectancy pattern with short RTs after continued runs of repetitions and alternations and long RTs when such runs are discontinued by the current stimulus. On a more general level, this expectancy effect can be described as a cost benefit pattern induced by a given higher order sequence as a function of the first-order sequence: If reaction times benefit from a specific preceding higher order sequence for one of the two first-order sequences, costs are incurred by the alternative first-order sequence.

The cost benefit pattern to be seen in RTs at long RSIs changes to a quite different pattern, however, when RSIs are shortened to 100 ms or less. In this case, preceding repetitions are always beneficial relative to preceding alternations, regardless of the first-order sequence. For example, higher order repetition runs will always produce comparatively short RTs as compared to alternation runs, whether being terminated by a first-order repetition or alternation. Depending on the point of view this pattern is termed benefit-only or—as adopted here—cost-only. Please note that such a pattern is different from what an expectancy account of sequential effects predicts. A change from a compatible stimulus-to-response mapping to a less compatible mapping delays the point of transition from a cost-only to a cost-benefit pattern with increasing RSI.

The cost-benefit and cost-only patterns as a function of the higher order sequence are usually accompanied by specific first-order sequence effects. At long RSIs, first-order alternations often yield shorter RTs than first-order repetitions (alternation effect), whereas at short RSIs, usually the opposite holds true, with first-order repetitions yielding shorter RTs than alternations (repetition effect). Note however, that there are numerous exceptions to this association of cost-benefit and first-order alternation effect on the one hand and cost-only and first-order repetition effect on the other hand (e.g. Bertelson & Renkin, 1966; Ford et al., 1982; Sommer et al., 1999).

Studies subsequent to the first report of sequential effects in ERPs have focused on the P300 component. In fact, the sequential effects and their explanation by expectancy mechanisms (Squires et al., 1976) have become one of the cornerstones in the most common account of P300, the context updating theory (Donchin & Coles, 1988; but Verleger, 1988). On the other hand, it is held by many researchers that P300 is not a single functional entity but more likely is a composite of more or less independent subprocesses. According to Johnson's (1986) model of P300 amplitude, sequential dependencies reflect a separate subprocess that contributes additively to the P300 amplitude with the effects of other factors such as task relevance or global stimulus probability. For example, independent effects of the stimulus sequence and global stimulus probability on P300 amplitude have already been reported by Squires et al. (1976) and Duncan-Johnson and Donchin (1977). In these studies, sequential effects on P300 amplitude were of the same magnitude for stimuli with high and low overall probabilities. Evidence of additive accounts of sequential effects to P300 amplitude also comes from studies with schizophrenic patients (Duncan-Johnson et al., 1984; Gonsalvez et al., 1995). In these patients, P300 is often globally diminished whereas the sequential effects are of the same size as in normal participants.

In more recent research, it has become apparent that the sequential effects in P300 amplitude and reaction time are not always correlated and sometimes may even dramatically dissociate. For example, P300 amplitude is usually smaller whereas RT may be longer for first-order repetitions as compared to alternations (Leuthold & Sommer, 1993; Sommer, Leuthold, & Matt, 1998). But also within the domain of higher order sequential effects, the correlation between P300 amplitude and reaction times appears to hold only for a restricted range of experimental conditions. Recently, Sommer et al. (1999) recorded ERPs in two-choice response tasks while manipulating the RSI. Whereas the sequential pattern in RTs changed from cost-benefit to cost-only when RSI was decreased from 500 to 40 ms, P300 amplitude consistently showed a cost-benefit pattern at both RSIs. Although sequential patterns in P300 amplitude did not change, the overall P300 amplitude was reduced in the short RSI condition. In line with the hypothesis of a sequence-specific P300 generator, P300 topography differed significantly between RSI conditions in such a way that the residual P300 in the short RSI condition showed a more anterior scalp distribution than in the long-RSI condition. Sommer et al. interpreted their results as confirming the suggestion that the P300 complex consists of several subcomponents. These subcomponents are functionally dissociable by their sensitivity to stimulus sequences as compared to other factors, but also by their scalp topography. Shortening RSI may specifically diminish sequence-insensitive parietally distributed subcomponents while sparing the sequence-sensitive subcomponent(s). If this hypothesis is correct, it should be possible to isolate the sequence-sensitive P300 subcomponent on the basis of its topographical properties from a sequence-insensitive subcomponent also in a long-RSI condition. This is a primary objective of the present study.

Because the putative subcomponents of P300 show widespread and highly overlapping spatial distributions, powerful methods are required for their spatiotemporal decomposition. To enhance the decompositional power of traditional principal components analysis (PCA), researchers have turned to increasing the number of electrode sensors (e.g., Spencer, Dien, & Donchin, 1999). This increase of spatial dimensions improves the chance for separating spatially orthogonal components. However, because P300 activity originates from a number of different brain areas most likely producing nonorthogonal scalp projections, an alternative approach is the development of nonorthogonal decomposition methods. In the present experiments, we have applied such a new method to the data, the Independent Component Analysis (ICA; Bell & Sejnowski, 1995; Makeig, Jung, Bell, Ghahremani, & Sejnowski, 1997). This method not only decorrelates the signals, as done by PCA, but also includes higher order statistical moments for the detection of functionally independent components and is able to deal with spatial overlap as long as the components are temporally independent. One of the advantages of this method is its ability to separate independent components even in data sets with a moderate number of electrodes. In simulation studies (Ghahremani, Makeig, Jung, Bell, & Sejnowski, 1996; Makeig, Jung, Ghahremani, & Sejnowski, 1996), ICA was able to correctly separate ERP components on the basis of only six sensors and was relatively insensitive to the location and orientation of simulated dipole sources within the brain. In a real ERP data set, ICA decomposition was relatively robust to the number and placement of electrodes by using arbitrary sets of 11 of the 14 recording channels (Makeig et al., 1997).

Using ICA, we assessed the hypothesis that there is a sequence-sensitive subcomponent of P300 that is separable from a more posterior sequence-insensitive subcomponent, to be seen particularly in long RSI conditions. The experiments of Sommer et al. (1999) had used spatially compatible stimulus–response (S-R) assignments in two stimulus modalities. It is conceivable that the peculiar scalp topography of the sequence-sensitive P300 subcomponent is specific for spatially defined stimuli. To assess the generality of the findings, a less compatible color-to-location mapping was used here as well.

In addition to separating ERP components on the basis of their scalp topography, it was a further aim of the present study to relate the components to putative underlying brain structures. In the past, many attempts have been made to localize P300 activity within specific brain regions. Findings from intracranial recording studies are summarized by Halgren, Marinkovic, and Chauvel (1998), demonstrating P300-like activity in multiple brain regions. The

authors proposed the existence of different cortical systems and their reflection in different aspects of P300. One system that is concerned with orienting of attention and originates in paralimbic as well as in the attentional frontoparietocingular cortex was related to the P3a or Novelty-P3. Cognitive contextual integration associated with P3b-like activity was related to activity in ventral temporofrontal event-coding cortices (inferotemporal, ventrolateral, and prefrontal), association cortices (superior-temporal and posterior-parietal structures) as well as the hippocampus. Kropotov and colleagues (Kropotov & Etlinger, 1999; Kropotov & Ponomarev, 1991) suggested that P300 may reflect a program selection mechanism and proposed a subcortical, thalamic contribution to the scalp-recorded P300.

The intracranial findings are in good correspondence with localization studies using noninvasive electrophysiological and hemodynamic measures recorded in standard oddball tasks. Clear hemodynamic or electrophysiological responses were found in superior-temporal regions (Ebmeier et al., 1995; Opitz, Mecklinger, von Cramon, & Kruggel, 1999; Yoshiura et al., 1999) and in the inferior parietal lobe (McCarthy, Luby, Gore, & Goldman-Rakic, 1997; Menon, Ford, Lim, Glover, & Pfefferbaum, 1997; Linden et al., 1999). Some authors also reported activity in cingulate (Ebmeier et al.; Menon et al.) and thalamic (Menon et al.) structures. In good accordance to these findings are results from equivalent dipole source models derived from scalp-recorded electric or magnetic P300 activity (Mecklinger & Ullsperger, 1995; Mecklinger et al., 1998; Tarkka & Stokic, 1998; Tarkka, Stokic, Basile, & Papanicolaou, 1995). In the present study, dipole source modeling of P300 subcomponents identified by prior ICA was undertaken.

Two experiments were conducted in order to induce different types of higher order sequential patterns in reaction time by varying the S-R mapping. Experiment 1 was spatially compatible and a cost-benefit pattern in RTs was expected. Experiment 2 used a less compatible stimulus color-to-response location mapping. Because decreasing compatibility at a given RSI may shift a cost-benefit pattern towards a cost-only pattern, a mixture of cost-only and cost-benefit in RTs was expected here. Independent of the pattern observed in RTs, a comparable cost-benefit pattern was predicted for P300 amplitude in both experiments.

EXPERIMENT 1

Method

Participants

A total of 10 participants (8 men) aged between 18 and 37 (mean: 26.8 years) were tested in this experiment. They were strongly right-handed, with handedness scores greater than +60 (Oldfield, 1971).

Stimuli and Procedure

Stimuli were white circular dots of 5 mm diameter, presented for 60 ms in random order and equiprobably 1 cm above or below a horizontal fixation line (4 mm in length) on the gray background of a computer monitor. Viewing distance was 1 m. The response onset-to-stimulus onset interval (RSI) was 700 ms. Responses were recorded with two keys mounted 15 cm behind each other in the midsagittal plane. The operation of the keys was assigned to the index fingers of the left and right hand, counterbalanced across participants.

Participants were instructed to press the top and bottom key in response to the dot above and below the fixation line, respectively. Responses were to be made both fast and accurately. A total of 3,960 stimuli was presented with a short break after each block of 330 trials during which information about mean RT and error rate was provided. Participants were advised to avoid eye movements and minimize eye blinks during the trial blocks.

Electrophysiological Recordings

The electroencephalogram (EEG) from the five midline sites Nosetip, Fz, Cz, Pz, and Oz, and the 27 lateral sites, IO1, IO2, FP1, FP2, F3, F4, F7, F8, F9, F10, C3′, C4′, C3, C4, T7, T8, T9, T10, M2, P3, P4, P7, P8, O1, O2, CB1, and CB2 was recorded with Sn electrodes and Beckman electrolyte paste with the left mastoid (M1) as common reference. For detecting electroocular (EOG) artifacts, the electrodes F9 and F10 were used as horizontal and the electrodes IO1 and FP1 as vertical EOG channels, respectively. All signals were amplified with a bandpass of 0–40 Hz (12 dB rolloff/octave) and digitized at a rate of 200 samples/s. The electrophysiological signals were continuously recorded together with markers for stimuli and responses. The exact electrode positions were measured using an OPTOTRAK system.

The continuous EEG record was separated into epochs of 1,000 ms duration synchronized with the stimulus event, containing 200 ms of prestimulus activity. For data analysis, only trials with correct key presses, RTs between 100 and 1,000 ms, and without EEG ($<80\ \mu V$) or EOG artifacts (ratio of covariance of blinks with template variance < 15) were considered. The first trial following an error also was excluded from data analysis. The waveforms were baseline corrected by subtracting the mean activity of a 200-ms prestimulus interval. An average reference montage was calculated for the activity at all EEG electrodes. Note that calculating an average reference recovers the initial common reference electrode (M1) as additional data channel. In a last step, the averaged ERPs were digitally low-pass filtered at 10 Hz (−3 dB).

Data Analysis

Each event was coded according to two responding hands and 16 different fourth-order stimulus sequences, disregarding the physical event and considering only whether it constituted a repetition or alternation with respect to its predecessor. We included responding hand as an additional factor mainly for stabilizing independent component analysis (S. Makeig, personal communication, 1999). For the analysis of sequential effects, we used the scheme of Soetens et al. (1985). The 16 sequences were subdivided into those for which the current stimulus was a repetition (R) or an alternation (A) of the immediately preceding stimulus (first-order sequences, FO). The eight higher order (HO) sequences for each first-order sequence were ordered as follows: RRR, ARR, RAR, AAR, RRA, ARA, RAA, and AAA, with recency increasing from left to right.

All dependent variables were subjected to repeated measures ANOVAs with factors First-Order Stimulus Sequence (R, A), Higher-Order Sequence (RRR to AAA), and Responding Hand (left, right). In the analyses of ERPs the factors Electrode and—if appropriate—Hemisphere were included as well (in the latter case the midline-electrodes were excluded). Note that because the average reference sets the mean activity across all electrodes within each condition to zero condition, effects in the ANOVA are only meaningful in interaction with electrode site. Therefore, only effects in interaction with electrode will be reported here; for ease of

presentation factor Electrode will not normally be mentioned. Conservative Huynh Feld-corrected F tests were used throughout.

The presence and type of sequential effects in a given dependent variable was assessed by comparing the slopes of the linear regressions across the eight higher order conditions between first-order repetitions and alternations. A typical cost benefit pattern is characterized by opposite slopes of the linear trends. In contrast, a cost-only effect is indicated by positive slopes for both first-order repetitions and alternations. Because of the average reference used here, the regression analyses for ERP amplitude measures were performed only at specific electrodes, usually at midline sites.

Independent Component Analysis

For the topographical analysis, the logistic "infomax" algorithm (Bell & Sejnowski, 1995, 1996; Makeig et al., 1997) was used to perform blind separation on the ERP data. Infomax ICA finds a square "unmixing" matrix by gradient ascent that maximizes the joint entropy (Cover & Thomas, 1991; Linkser, 1992; Nadal & Parga, 1994) of a nonlinearly transformed ensemble of zero-mean input vectors; for details of the method see Makeig et al. (1999). In the present study ICA was based on the grand mean data of 32 conditions (16 sequential Conditions × 2 Hands × 200 Time Points) across all participants. In factor-analytic terminology, ICA decomposition results in functionally independent factors with different factor loadings for each electrode site. The sum of the factors weighted with its loadings at any specific time point and condition yields the scores. The activation functions used in this paper resulted from plotting these scores as a function of time. It is important to note that like spatial PCA, ICA does *not* imply the same time course of activation for all experimental conditions as does temporal PCA. Rather, a given spatially defined component may show different time courses—and thus latencies—for different conditions. For statistical assessment of sequential patterns in the ICA components, the decompositions of the grand mean data were reprojected into the ERPs of each participant, yielding a score for each ICA component, participant, and condition, which was then submitted to the same type of ANOVA as the performance data and ERP amplitudes.

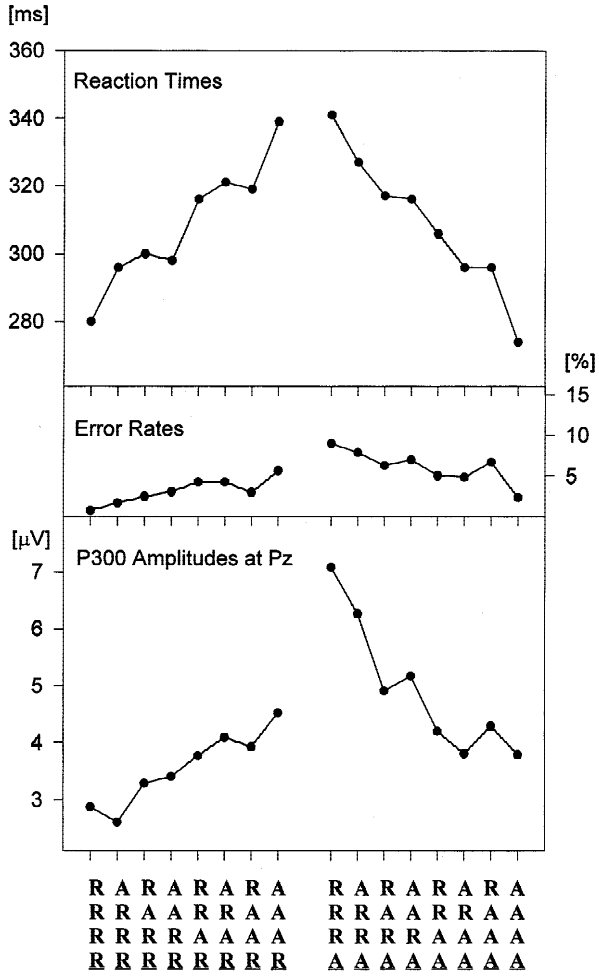

Figure 1. Sequential effects for Experiment 1 in reaction times (top), error rates (middle), and P300 amplitude at the Pz electrode (bottom). The variables are plotted as a function of first-order repetitions and alternations of the preceding stimulus (R and A, left and right side of each panel, respectively) and the eight higher order sequences within each first-order sequence, ordered from three repetitions (RRR) to three alternations (AAA).

Results

Performance

Figure 1 (top) shows the expected cost-benefit pattern in RTs, statistically confirmed by a significant interaction of higher order and first-order stimulus sequence, $F(7,63) = 30.1$, $p < .001$. This holds true also for the interaction of the linear trend for FO × HO, $F(\text{linear:}1,9) = 44.1$, $p < .001$. No other effects in RTs were significant.

Fewer errors (Fig. 1, middle) were made for first-order repetitions as compared to alternations ($M = 3.3$ vs. 6.3%), $F(1,9) = 21.8$, $p < .001$. The higher order sequences interacted with the first-order stimulus sequences, $F(7,63) = 26.9$, $p < .001$; $F(\text{linear: } 1,9) = 85.6$, $p < .001$, but showed no main effect. The interaction of FO with HO was more pronounced for right-hand responses, as indicated by a significant interaction Hand × FO × HO, $F(7,63) = 2.2$, $p < .05$; $F(\text{linear: } 1,9) = 6.1$, $p < .05$.

ERP Amplitudes

Figure 2 shows the ERP wave shapes for the most extreme stimulus sequences. Mean P300 latency at the Pz electrode was 355 ms. P300 amplitude was measured as average ERP voltage between 300 and 400 ms after stimulus onset. As expected, P300 amplitude was maximal at centroparietal electrode sites, $M(\text{Fz, Cz, and Pz}) = 2.2$, 6.4, and 4.3 μV, respectively. P300 amplitude showed the typical FO repetition effect (Figure 1, bottom), $F(32,288) = 7.6$, $p < .001$, and a cost benefit pattern, indicated by a significant HO × FO interaction, $F(224,2016) = 7.6$, $p < .001$, including opposite linear trends at the Pz electrode, $F(\text{linear: } 1,9) = 56.1$, $p < .001$.

Interestingly, there was a significant interaction Hand × FO × HO × Hemisphere, $F(91,819) = 3.1$, $p < .01$. As suggested by Figure 3, this interaction is due to a more pronounced cost benefit pattern at electrodes ipsilateral to the responding hand as compared to contralateral electrodes. The same holds true for the interaction of the first-order repetition effect with Hand and Hemisphere, $F(13,117) = 17.2$, $p < .001$. Both effects were maximal over the C3 and C4 electrodes.

ICA Decomposition

Component identification was restricted to a time segment of 250 to 450 ms after stimulus onset where P300 activity is maximal and

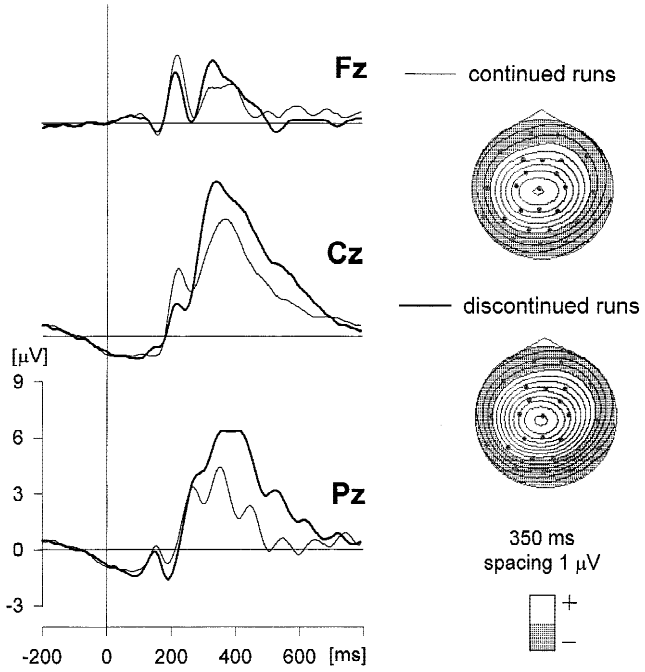

Figure 2. Grand mean ERP waveforms of the discontinued (RRRA, AAAR) and continued (RRRR, AAAA) runs of stimulus repetitions and alternations together with the spline maps of the ERP amplitudes at 350 ms after stimulus onset for Experiment 1.

where contributions of postmovement potentials are still small, considering our short reaction times. In the interval examined, only three ICA components accounted for nearly all of the variance (96%) in the data (Figure 4). Amplitude effects in each component were calculated as a mean amplitude score of a 50-ms interval around its mean peak latency.

The largest share of variance was explained by ICA Components 1 and 2 (44 and 43%, respectively). Both components were maximally positive over central electrode sites and peaked with a latency of about 360 ms. Interestingly, both components showed hand specificity because each was present mainly in trials where either the right or left hand but not the other hand responded, confirmed by significant effects of factor Hand in the ANOVAs of the ICA component scores, $Fs(1,9) = 25.3$ and 19.5, respectively, $ps < .01$. ANOVA also confirmed the presence of a cost-benefit pattern in interaction with responding hand, $Fs(\text{linear: } 1,9) = 10.6$ and 3.3, $ps < .01$ and $< .1$. Testing only for the hand where the components are active, significant cost-benefit patterns were found for right-hand responses in Component 1 and left-hand responses for Component 2, $Fs(\text{linear: } 1,9) = 18.3$ and 12.7, $ps < .01$. In addition, there was a significant effect of the first-order sequence for Component 1 with larger amplitudes for alternations than repetitions, $F(1,9) = 6.5$, $p < .05$.

Importantly, a third ICA component (#3) was found within the 250—450-ms interval after stimulus onset that explained 9% of the variance in the data and peaked with a latency of 295 ms. This component showed a bilateral distribution that was more posterior than that of Components 1 and 2. Component 3 was not hand specific and did not show any sequential effects ($p > .1$).

Discussion of the First Experiment

Experiment 1 induced the expected cost benefit pattern in performance. The sequential effects in RTs cannot be explained by a speed–accuracy trade-off because the error rates showed this pattern as well. Interestingly, there was no first-order alternation

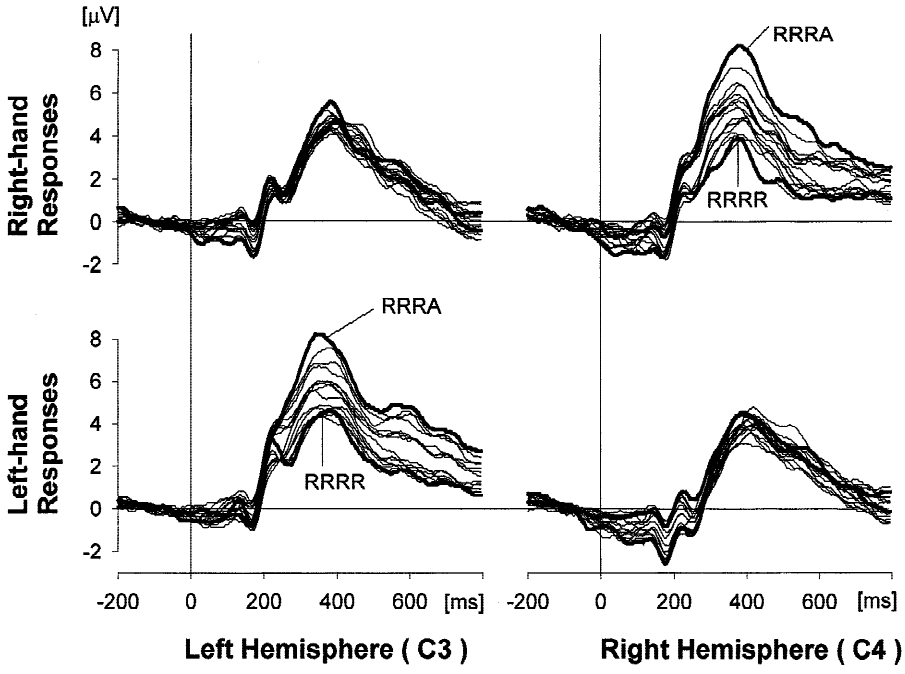

Figure 3. ERPs from all 16 sequence conditions as a function of responding hand, recorded above left (C3) and right (C4) motor cortex for Experiment 1.

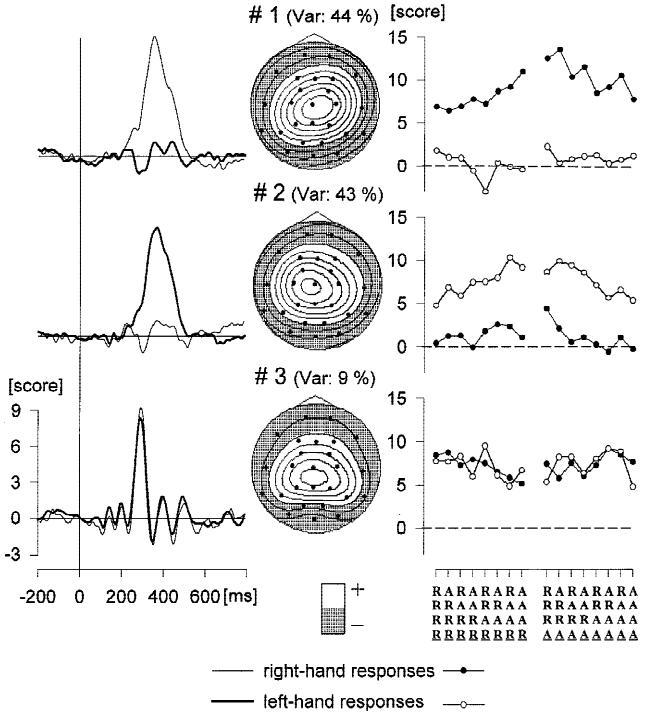

Figure 4. ICA decomposition of ERPs in the P300 time range from Experiment 1: time-course (left), scalp topographies (middle), and sequential patterns (right) of the ICA components.

effect as is sometimes observed in spatially compatible conditions with long RSIs even when there is a higher order cost-benefit pattern (e.g., Soetens et al., 1985; Sommer et al., 1999, Exp. 1).

Replicating earlier studies, we found the typical cost benefit pattern also in the amplitude of a centroparietal P300, that is, opposite slopes across higher order sequences for the two first-order sequences. The data also displayed the often-reported first-order repetition effect in P300 amplitude. A hitherto unobserved finding was the lateralization of both the cost-benefit pattern and the first-order repetition effect in P300 amplitude towards the hemisphere ipsilateral to the responding hand.

The ICA decomposition of the ERPs confirmed the sequential effects and the hand relatedness observed in the amplitude analyses but was able to relate them to topographically specified subcomponents in the P300 time range. ICA separated two sequence-sensitive subcomponents (#1 and #2) with a widespread central distribution from a parietal and bilaterally distributed sequence-insensitive component (#3). Because of their timing and polarity, all three components qualify as subcomponents of the P300. As Johnson (1993) pointed out, the P300 component is not restricted to a specific topography because different task-dependent generators are contributing to P300 activity as a whole. In the present study, it is not Component 3 with its parietal scalp distribution that shows the P300-typical higher-order cost-benefit effect. These effects appear in the more central Components 1 and 2. Most generally, this finding is in line with the hypothesis of distinct subprocesses constituting the P300 component, indicated by the additivity of sequential influences and other factors to P300 amplitude at large (Johnson, 1988). More specifically, the dissociation of a sequence-insensitive and a sequence-sensitive positive-going subcomponent in the P300 time range directly confirms the hypotheses of Sommer et al. (1999), based on a comparison of ERPs from different RSI conditions.

EXPERIMENT 2

Experiment 1 demonstrated a cost-benefit pattern in nonparietal subcomponents of P300 in a long-RSI condition, confirming the hypothesis of Sommer et al. (1999). These authors had reported a dissociation between a robust cost-benefit pattern in P300 amplitude and reaction times when RSI was decreased to 50 ms. In the latter condition, RTs showed a so-called cost-only or benefit-only pattern. This finding was seen as conforming the suggestion of Sommer et al. (1998) that the mechanism underlying the sequential effects in P300 are nonconscious and automatic. Therefore it would be interesting to assess whether the stimulus sequence-related subcomponents extracted here by ICA would be robust and dissociable from sequential effects in RTs. Unfortunately, decreasing RSI as done by Sommer et al. (1999) has the disadvantage of inducing massive temporal overlap between the ERPs elicited by subsequent events. In the present study, a different approach was taken in order to dissociate RTs from ERPs. As mentioned in the Introduction, reducing the stimulus-response compatibility strengthens the contribution of cost-only patterns to the sequential effects in RTs. Therefore, while maintaining a long RSI, a less compatible S-R mapping was chosen for Experiment 2 that should shift the RT pattern towards cost-only. If the ERP findings reported in Sommer et al. (1999) generalize to this condition, we should expect a cost-benefit pattern in an ERP component anterior to Pz in this experiment as well.

Method

A total of 10 participants (4 men), aged between 20 and 28 (mean: 24.4 years) were tested in this experiment. They were strongly right-handed, with handedness scores greater than +60. Stimuli were red or green dots (diameter 5 mm) appearing in the center of the monitor. Each color was assigned to one of the keys. The assignment of finger to key and key to color was counterbalanced over participants. Otherwise the method was the same as in Experiment 1 using the long RSI of 700 ms. A fixation point was always present in the center of the monitor.

Results

Performance

Reaction times (Figure 5, top) were affected by higher order sequences both as a main effect, $F(7,63) = 15.0$, $p < .001$; $F(\text{linear: } 1,9) = 21.4$, $p < .01$, as well as in interaction with the first-order sequences, $F(7,63) = 27.4$, $p < .001$; $F(\text{linear: } 1,9) = 55.0$, $p < .001$. These effects were accompanied by a first-order repetition effect, that is, faster reactions to repetitions as compared to alternations, $M(\text{R vs. A}) = 354$ vs. 404 ms, $F(1,9) = 82.4$, $p < .001$.

As in the first experiment, less errors were made for first-order repetitions than alternations, $M(\text{R vs. A}) = 4.2$ vs. 7.2%, $F(1,9) = 10.6$, $p < .01$. There was a main effect of the higher order stimulus sequence, $F(7,63) = 8.0$, $p < .001$; $F(\text{linear: } 1,9) = 16.0$, $p < .01$, as well as an interaction with first-order sequences, $F(7,63) = 13.0$, $p < .001$; $F(\text{linear: } 1,9) = 26.0$, $p < .001$ (Fig. 5, middle).

ERP Amplitudes

P300 at the Pz electrode (Figure 6) peaked at 375 ms and the average amplitudes (325–425 ms) showed a centroparietal scalp

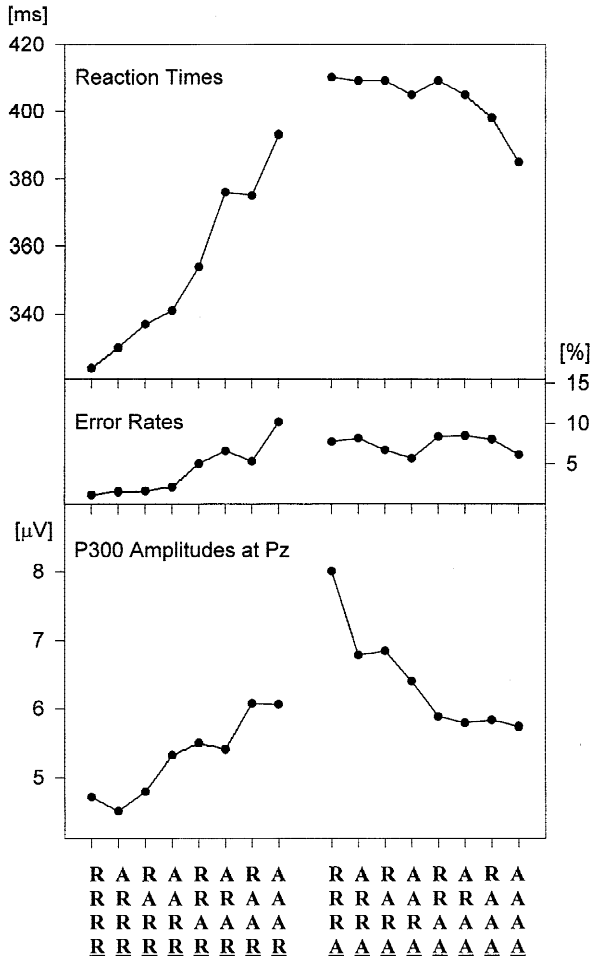

Figure 5. Sequential effects for Experiment 2 in reaction times (top), error rates (middle), and P300 amplitude at the Pz electrode (bottom).

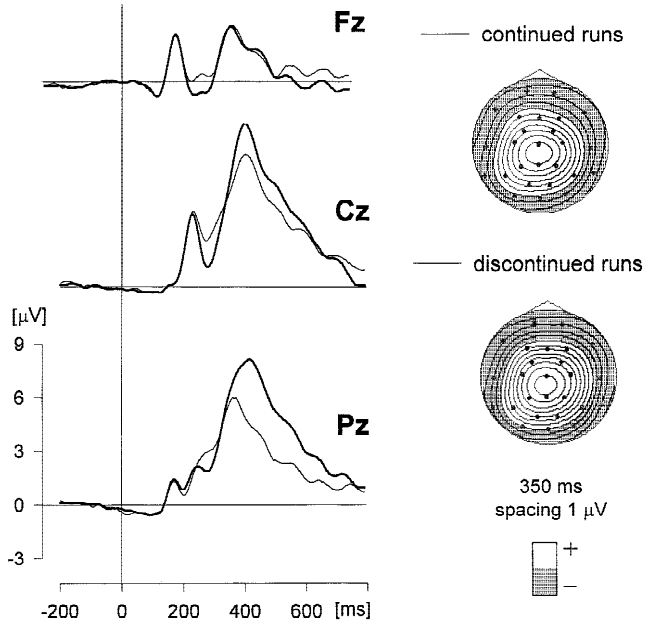

Figure 6. Grand mean ERP waveforms of the discontinued (RRRA, AAAR) and continued (RRRR, AAAA) runs of stimulus repetitions and alternations together with the spline maps are drawn at 350 ms after stimulus onset for Experiment 2.

topography, M(Fz, Cz, and Pz) = 2.0, 6.8 and 5.8 μV, respectively. As can be seen in Figure 5 (bottom), P300 amplitude showed the usual cost-benefit pattern (HO × FO), $F(224,2016) = 7.5$, $p < .001$, F(linear at Pz: 1,9) = 52.4, $p < .001$, as well as the first-order repetition effect, $F(32,288) = 5.5$, $p < .01$.

As in Experiment 1, there was also a significant interaction Hand × FO × HO × Hemisphere, $F(91,819) = 2.0$, $p < .05$. As suggested by Figure 7, this finding is due to a more pronounced cost-benefit pattern at the hemisphere ipsilateral to the responding hand as compared to contralateral electrode sites. The same ipsilateral preponderance holds true for the first-order repetition effect Hand × FO × Hemisphere, $F(13,117) = 12.5$, $p < 0.001$. Again, the effects were maximal over the C3 and C4 electrodes.

ICA Decomposition

Confirming the results of Experiment 1, ICA decomposition of the ERP data from this experiment again resulted in three subcomponents that explained most of the variance (95%) within the P300-related 250 to 450-ms time interval after stimulus onset (Figure 8). Again amplitude effects in each components were calculated as a mean amplitude score of a 50-ms interval around peak latency. The ICA Components 1 and 2 that accounted for the largest share of the variance (45 and 39%, respectively) peaked at about 400 ms after stimulus onset and showed positive maxima over central electrode sites. Both components showed hand specificity because each was present only for trials where either the right or left hand but not the other hand responded, $Fs(1,9) = 23.1$ and 17.6, $ps < .01$. ANOVA of the scores of these ICA components confirmed the presence of a cost-benefit pattern in interaction with responding hand, Fs(linear: 1,9) = 5.1 and 25.1, $ps < .05$. When testing only the hand where the components are active there were significant cost-benefit patterns for right-hand responses in Component 1 and for left-hand responses in Component 2, Fs(linear: 1,9) = 11.5 and 30.8, respectively, $ps < .01$. In addition, there was a significant first-order sequence effect for Component 1 with larger amplitudes for alternations than repetitions, $F(1,9) = 22.6$, $p < .001$.

As in Experiment 1, ICA also extracted a further component (#3) within the P300 time range that still explained 11% of the data variance in the 250 to 450-ms interval. This component showed a mean peak latency of 320 ms (Figure 8, bottom), a more posterior scalp distribution than the first two components, and it was lateralized to the left hemisphere. Component 3 was not hand specific and neither first-order nor higher order sequential effects were found to be significant in this component.

Discussion of the Second Experiment

RTs and error rates were similarly affected by higher order and first-order sequences as well as by their combination. Thus performance as a whole indicated the presence of both a cost-benefit and a cost-only pattern as a function of the stimulus sequence. This is the predicted result of using a less compatible color-to-location stimulus-response assignment compared to Experiment 1 where the assignment was spatially compatible and results showed a clear cost-benefit pattern.

Conforming with the findings of Experiment 1, the stimulus sequences in Experiment 2 also yielded a cost-benefit pattern in

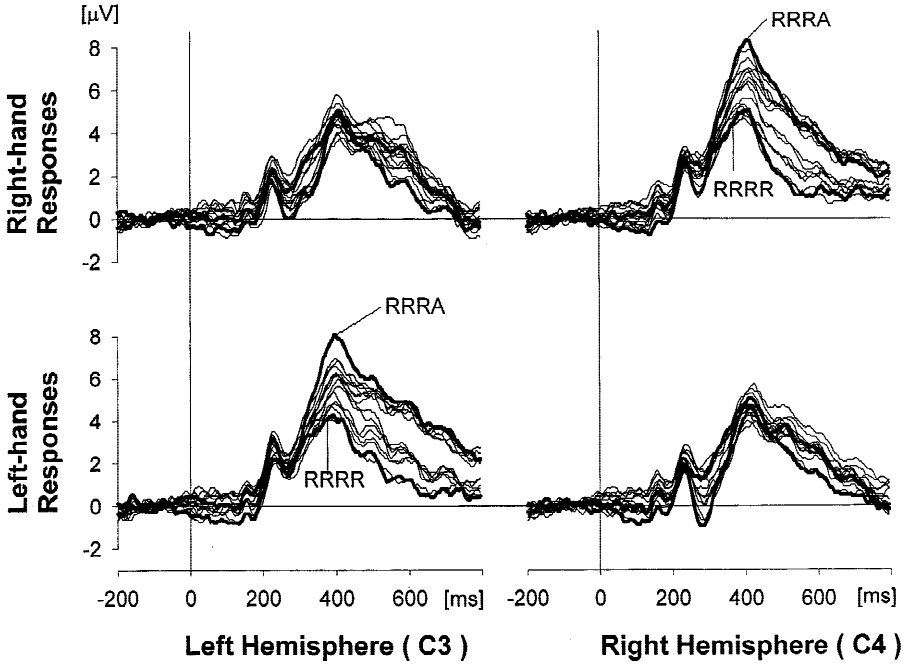

Figure 7. ERPs from all 16 sequence conditions as a function of responding hand, recorded above left (C3) and right (C4) motor cortex for Experiment 2.

P300 amplitude. Therefore, the findings of a stable cost-benefit pattern can be extended to experiments using not space but color as relevant visual stimulus dimension. The unexpected finding of Experiment 1 that the cost-benefit pattern as well as the first-order repetition effect is at least partially lateralized as a function of response hand could be replicated in this experiment. Basically in line with the findings of Experiment 1, ICA separated two sequence-sensitive and hand-specific centrally distributed P300 subcomponents from a more parietal sequence-insensitive P300 component.

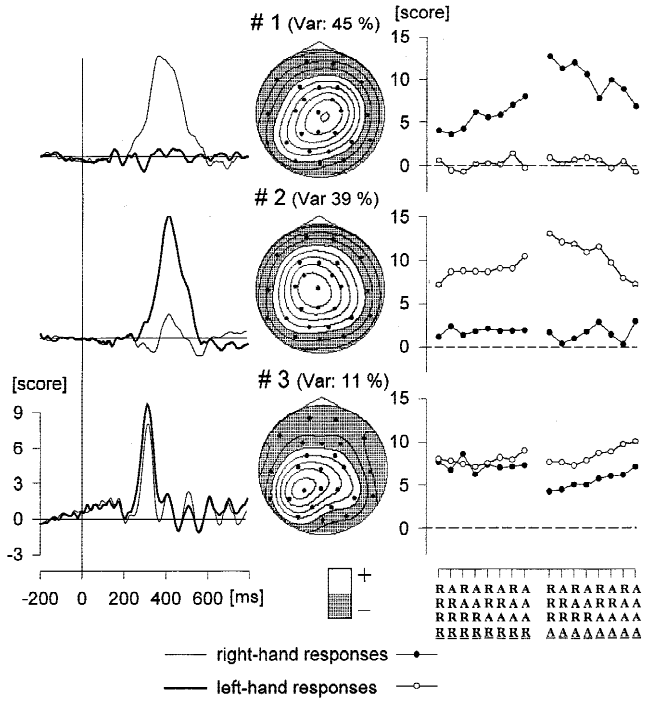

Figure 8. Largest ICA component extracted from the ERPs of Experiment 2: time-course (left), topographic maps (middle), and sequential pattern (right).

GENERAL DISCUSSION

In both experiments with spatial and nonspatial stimulus arrangements, sequence-sensitive ERP components in the time range of P300 were extracted by means of ICA that were separate from a slightly earlier but more posterior and sequence-insensitive positivity. Interestingly, the sequence-sensitive component showed hand specificity. In the following, discussion will focus on these two main findings. In a subsequent section we will present dipole localization of the observed ICA components.

As previously reported many times, the P300 component showed the typical cost-benefit pattern as a function of the preceding stimulus-response cycles. For example, larger amplitudes were obtained for discontinued runs of alternations and repetitions and smaller amplitudes for continued runs of repetitions and alternations. In line with recent findings (Sommer et al., 1999), a stable cost-benefit pattern in P300 was observed for two experiments yielding different patterns in overt performance. The current Experiment 2 shows that a stable cost-benefit pattern in ERPs emerges when a spatial noncompatible mapping of color-to-response location had been employed, yielding a mixture of cost-benefit and cost-only patterns in reaction times. The dissociability of the sequential effects in performance and in P300 support the suggestion of Sommer et al. (1998) that the mechanism that generates sequential effects in P300 amplitude operates at a relatively automatic level of the information-processing system. This mechanism has traditionally been seen as some sort of expectancy for the continuation of an ensuing repetition or alternation pattern. It has

been suggested that discontinuation of the pattern by the current stimulus is surprising and elicits a larger P300 (Squires et al., 1976) together with long RTs. The robustness of cost-benefit effects in P300 amplitudes even at short RSIs as observed by Sommer et al. (1999) was taken to indicate that the sort of expectancy mechanism underlying the sequential effects in P300 requires little resources. Other findings supporting the suggestion of Sommer et al. (1998) that sequential effects in P300 are automatic and unconscious are their insensitivity to induced expectancies (Matt, Leuthold, & Sommer, 1992) and the extremely limited relation between self-reports of expectedness and the preceding stimulus sequence (Sommer et al., 1990). In contrast to P300 amplitude, the sequential effects in reaction times have been shown to be considerably more variable. They are not only sensitive to the RSI and the S-R compatibility as has been shown here but also to voluntary strategies of the participant (Matt et al., 1992). Together these findings indicate that sequential patterns in RT are influenced by many more factors than the patterns in P300 amplitude.

The present findings that the sequence-sensitive subcomponent of P300 is not identical with the classical parietally distributed P3b even at long RSIs is broadly in line with the idea that there is a separate low-level sequence-sensitive P300 generator. Note that the present findings about the first-order effects are also in agreement with this idea. Whereas the components sensitive to the higher order sequences also showed clear first-order repetition effects (whether or not first-order effects appeared in RTs), no such effects appeared in the sequence-insensitive components.

Sommer et al. (1999) observed that—although sequential effects are unaltered—as RSI decreases, P300 amplitude is globally diminished and shows a different scalp topography than at long RSIs. Therefore, it was suggested that at the long RSIs normally employed, P300 consists of parietal sequence-insensitive and more anterior sequence-sensitive subcomponents. Moreover, decreasing RSI attenuates the parietal component(s) but spares the more anterior component. Because these conclusions rested on the short-RSI ERPs that were corrected for temporal overlap by adjacent ERPs with a complex method (Woldorff, 1993), it is important to have obtained further independent evidence in the present study. According to the hypothesis of Sommer et al., it should be possible to separate these subcomponents of P300 also in a long-RSI condition, suitable methods provided. With the small number of electrode sites used by Sommer et al., this was not possible because of the strong spatial overlap between the putative subcomponents. Therefore, the present experiments attempted to separate subcomponents of the P300 by recording multichannel ERPs and applying the ICA method.

Confirming the hypothesis of Sommer et al., it was possible to separate by means of ICA sequence-sensitive P300-like subcomponents from a sequence-insensitive component in both experiments. On average, the sequence-dependent components peaked later and showed more anterior maxima and more widespread topography than the sequence-insensitive subcomponent. This topographical difference in the anterior–posterior direction becomes especially clear at the recording sites to the left and right of the midline.

On a general level, the topographical separation of subcomponents in the P300 time range with specific sensitivity to experimental manipulations supports the suggestion of Johnson (1993) that P300 consists of multiple subcomponents differing in functional significance and originating in different brain areas. The sequence-insensitive ICA component shows a parietal distribution in line with the often reported Pz-maximum of the classical P300 component as observed, for example, in response to rare target stimuli. Although the present experiments do not provide direct evidence of the significance of the parietal ICA component apart from its insensitivity to stimulus sequences, it is tempting to speculate that the parietal component may reflect the lion's share of what is usually termed the P3b component, whereas the more anterior sequence-sensitive components are separate phenomena.

However, recent findings also suggest alternative accounts of the parietal ICA component. Thus, it might reflect event-synchronized oscillatory activity as discussed by Yordanova, Devrim, Kolev, Ademoglu, and Demiralp (2000). These authors reported that especially delta, theta, and alpha time-frequency components of the EEG depend on similar factors as those that elicit P300. An account of the parietal ICA component in terms of oscillatory activity is also in line with a so-called P1r (P100 reprise) component, reported by Tucker, Liotti, Potts, Russell, and Posner (1994), which might be a reflection of some sort of corticothalamic oscillation. Because little is known about the functional significance of the P1r or oscillation-related contributions to P300, future research should be aimed at delimiting the relative contributions of the alternative explanations of the parietal ICA-determined subcomponent.

Both in the ERP waveforms and in the ICA components the sequence-sensitive P300 component was lateralized to the hemisphere ipsilateral to the response hand. That is, at central electrode sites ipsilateral to the responding hand there were much stronger sequential effects as compared to the homologous contralateral sites. Although replicable, the observation of hand-related lateralization of sequential effects in ERP components has never been reported previously. We suspect that this is due to a combination of two factors. For one, studies of sequential effects in ERPs have usually used only midline electrode sites. Second, on the assumption that lateralization of sequence-dependent ERPs depend on manual bilateral responses, it may not have been present in many previous studies of sequential effects because they have employed counting tasks.

There are several conceivable explanations for the hand-related lateralization of the sequential effects in the present experiments. For one, overlap of different processes might contribute to this pattern. The sequence-sensitive P300 subcomponent might be broadly distributed and symmetric over both hemispheres but may be overlapped by a negative-going ERP component at contralateral sites that is also sequence sensitive (see Figure 9). In this case, the topographical differences resulting from left- and right-hand related movement potentials would force ICA to split the potentials into two hand-specific components.

A possible candidate for a negative-going component overlapping with P300 is the readiness potential that is more pronounced above the hemisphere contralateral to the response hand (e.g. Coles, 1989). On the assumption that the readiness potential is also sequence-sensitive, the positive-going P300 and the negative-going readiness potential might partially cancel above the contralateral hemisphere, leaving only the residual P300 above the ipsilateral hemisphere. In line with such an hypothesis is the idea of overlapping contributions of movement-related potentials within the P300 time range (Kok, 1988) especially in the case of relatively fast responses.

Alternatively, the ipsilateral sequential effects in P300 may be the result of a process that inhibits the nonrequired response that is governed by the hemisphere ipsilateral to the required response. Speculatively, such a inhibitory process reflected by P300 amplitude might be related to a positivity over ipsilateral motor areas

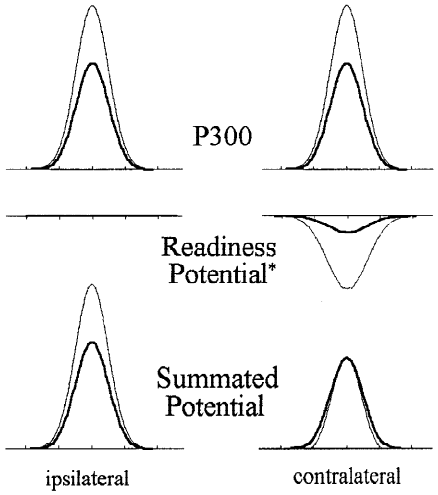

Figure 9. Idealized model for explaining the lateralization of sequential effects in P300 towards the side ipsilateral of the response hand by overlap with contralateral readiness potential or—more generally—movement-related activity (*for ease only, the contralateral dominating part of this potential prior to response execution is shown). Thick and thin lines depict sequential effects.

and costs for inhibition might differ according to the preceding sequence. Although some authors suggest that response suppression contributes to P300 amplitude (Roberts, Rau, Lutzenberger, & Birbaumer, 1994), there is little neurophysiological evidence for such inhibitory processes. Neither in premotor areas (Weinrich, Wise, & Mauritz, 1984) nor in primary motor areas (e.g., Miller, Riehle, & Requin, 1992) has cell activity related to motor inhibition been found. In the following section these explanations are further investigated.

Dipole Source Localization

After having consistently separated sequence-sensitive from sequence-insensitive subcomponents within the P300 time range by means of ICA in two experiments, it appeared to be of interest whether these components might be related to specific underlying brain structures. Another interesting question was the hypothesis of motor-related contributions producing the hand specificity of the sequence-sensitive subcomponents. In the following, both questions were pursued by applying brain electric source analysis (BESA; Scherg & Berg, 1996) to the ICA components extracted in the preceding experiments.

Dipole modeling of the sources of the ICA components was performed by using the BESA method (Version 2.2; Scherg & Berg, 1996). On the basis of a four-shell spherical head model, fixed dipoles were fitted in the time intervals of 250 to 450 ms after stimulus-onset by minimizing residual variance. An energy criterion of 20% was used to avoid interactions between dipoles.

In a first step, the sequence-sensitive subcomponents (#1 and #2) were fitted separately. From the hypothesis formulated above, movement-related contributions were expected for these components. Therefore a model of movement-related activity was derived as described in the Appendix, and applied to the data of the two ICA components. Modeling started with adding to the movement-related model one additional dipole pair, which was symmetric in location as well as orientation in both hemispheres. Please note that despite these symmetries, the additional dipoles are still capable of modeling asymmetric scalp distributions due to possible independent variations of source strength in each hemisphere. The additional dipole pair was fitted freely by holding the movement-related dipole pairs fixed. The resulting dipole models for the first two components in each experiment are shown in Figure 10.

In a second step, the sequence-insensitive ICA components of the two experiments were modeled separately. Modeling started with freely fitting a single symmetric dipole pair. In both data sets, the residual variance was still larger than 10%; therefore, a second dipole pair was added and both pairs were fitted again. The resultant solutions (Figure 11) yielded residual variances of 1.2 and 6.2%, respectively, for the two experiments.

In a final step the models for the three different ICA components were combined to assess the power of the composite solutions to explain the activity during the P300 time range (250 to 450 ms) in the original ERP wave shapes. Because the movement-related dipoles in the models for ICA Components 1 and 2 (i.e., Dipoles 1 to 4 in Figure 10) are identical, the resulting composite model consisted of six dipole pairs, being symmetric in location and orientation. Consistently across experiments, the additional dipole pair for ICA Components 1 and 2 (Dipoles 5 and 6) was located in nearly identical brain regions, differing only in hemispheric asymmetry. Therefore, the mean of these two dipole pairs was used for the composite model, reducing the total number of dipole pairs to five per experiment. The final composite model for each experiment consisted of two movement-related pairs (Dipoles 1 to 4 of Figure 10), the additional dipole pair for the sequence-sensitive ICA components (Dipoles 5 and 6 of Figure 10), and two pairs for the sequence-insensitive ICA component (Dipoles 1 to 4 of Figure 11). The resulting composite dipole model of each experiment was projected into the corresponding grand mean ERP data set and the residual variance was calculated without any further fitting, amounting to 1.6 and 2.1%, respectively.

The composite models derived from each experiment provided good explanations also for the data of the *other* experiment. Thus when the data of Experiment 1 were modeled with the dipoles derived from Experiment 2, the residual variance was still only 2.1%, and when the ERPs of Experiment 2 were modeled with the dipoles from Experiment 1, it was 3.4%.

Discussion of the Dipole Source Analysis

In the present study, ICA decomposition was combined with dipole source analysis to localize the sequence-sensitive subcomponent of P300 and to assess the hand specificity of the sequence-sensitive ICA components. We concluded from the results of the two experiments that five bilateral sources of activity in the time range of P300 could be extracted by combining ICA decomposition and inverse dipole modeling. Sequence-insensitive activity was found to be located mainly in parietal but also in superior temporal brain regions. The components showing sequence sensitivity were consistently localized in more mesial and more anterior brain regions and included also movement-related activity.

The results strengthen the hypothesis that the lateralization of sequential effects in P300 time range as reflected in the hand specificity of ICA components 1 and 2 might be related to overlap with motor potentials. As seen from Figure 10, in Experiment 1 lateralized sequence-sensitive ERP activity is accounted for by movement-related dipoles whereas an additional symmetric contribution to sequence-sensitive activity to the P300 amplitude arises from deeper mesial brain regions. In Experiment 2 this contribution is not symmetric, but dominant in the left hemisphere. Interestingly, postmovement activity, presumably related to reafferent

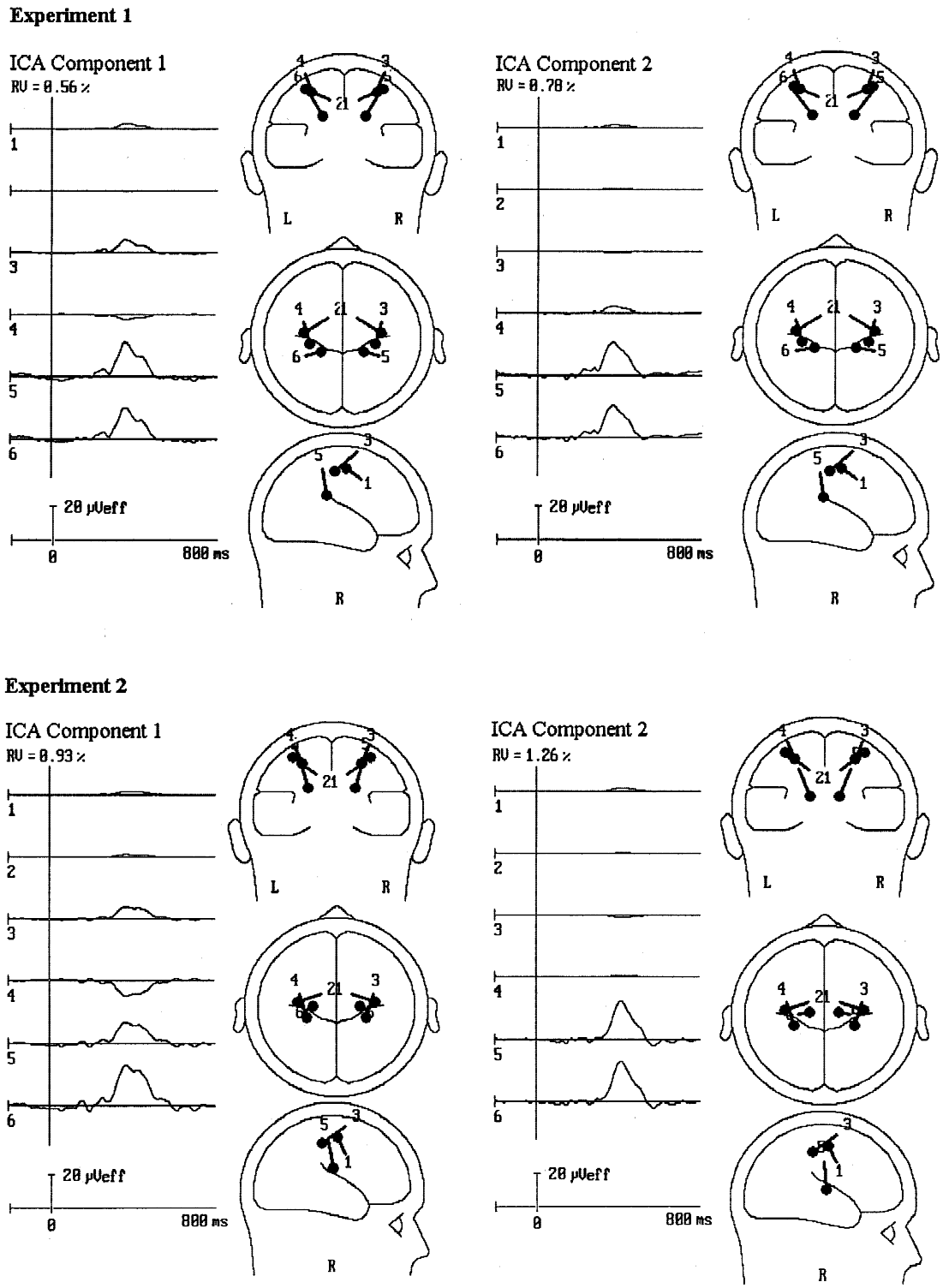

Figure 10. Dipole solutions (source waveforms and dipole locations and orientations) for the *sequence-sensitive* ICA Components 1 and 2 (left vs. right panel) for Experiments 1 and 2 (top vs. bottom figure). In each model, Dipoles 1 to 4 explain movement-related activity, whereas Dipoles 5 and 6 show additional activity required to model these ICA components.

processes (Dipoles 3 and 4), contributes much more to the model than the earlier primary motor activity (Dipoles 1 and 2). Therefore primary motor-cortex activity does not appear to be responsible for producing the hand specificity of the sequence-sensitive ICA components. Rather, there appears to be a substantial contribution by asymmetric reafferent activity possibly arising from somatosensory areas. Therefore ICA Components 1 and 2 may indeed result from overlapping and inseparably related activity

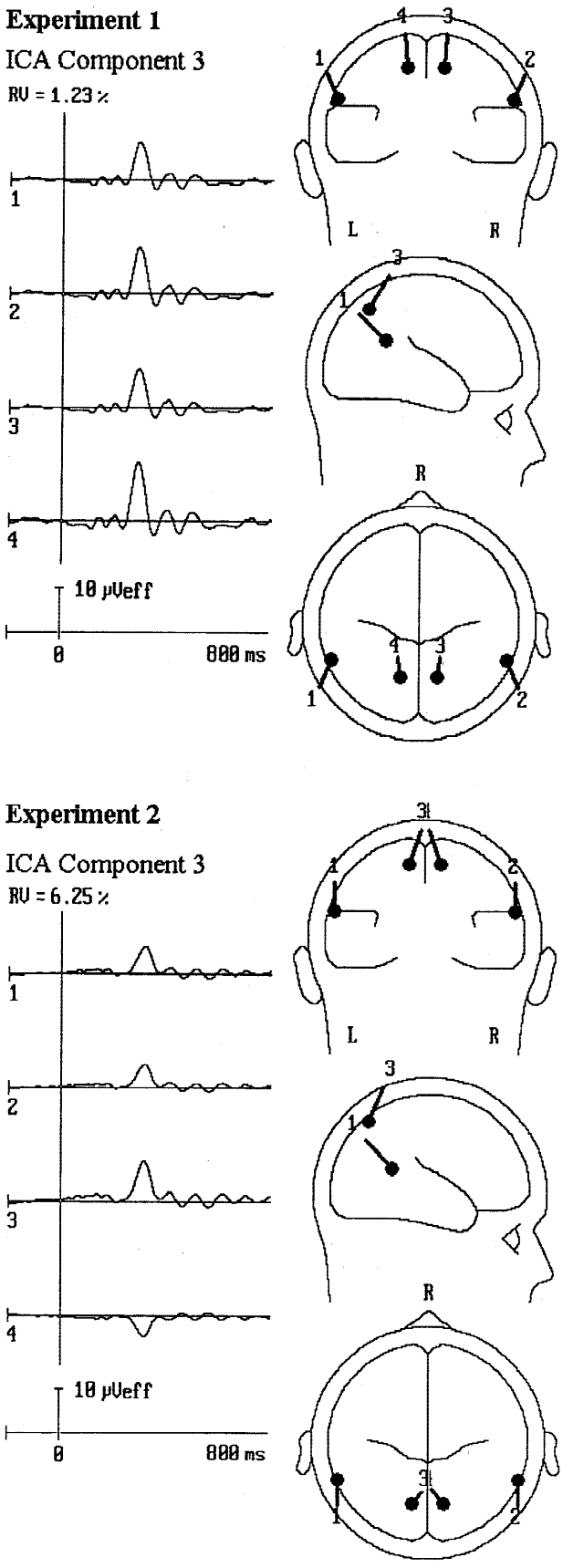

Figure 11. Dipole solutions (source waveforms and dipole locations and orientations) for the *sequence-insensitive* ICA components of Experiments 1 and 2.

originating from different generator locations within the brain, a symmetric sequence-sensitive P300 overlapped by a likewise sequence-sensitive reafferent potential whose asymmetry is hand related.

The sequence-sensitive nonmotoric aspect of P300 was localized in deep mesial brain regions, indicating a source in subcortical, possibly thalamic or cingulate cortex areas. Similar findings, indicating mesial subcortical or cingulate contributions to P300 have been reported also by others (e.g. Ebmeier et al., 1995; Kropotov & Etlinger, 1999; Kropotov & Ponomarev, 1991; Mecklinger et al., 1998; Menon et al., 1997; Rogers et al., 1991). However, because of the limitations of inverse modeling it cannot be ruled out that the deep location of the sequence-sensitive dipole is due to a very widespread cortical activation. Nevertheless the results clearly show that different generators within the brain contribute to sequence-sensitive and -insensitive aspects of the late positive complex.

The sequence-insensitive activity of ICA Component 3 was localized in parietal and in superior-temporal brain regions, in line with results of combined ERP/fMRI studies (e.g. Menon et al. 1997) and intracranial recordings (e.g., Halgren et al. 1998) for the oddball-elicited P300. This correspondence in equivalent dipole localization strengthens the idea that the parietal ICA component may in fact relate to aspects of the classical P3b component. In contrast, the dipoles reported for one of the alternative accounts of the parietal component, the P1r, are located quite differently (Dien, 1999), which makes this explanation less plausible. In addition, the scalp distribution of P1r was lateralized to the right hemisphere whereas the present ICA Components #3 were, if anything, lateralized to the left side. Moreover, Dien related the P1r to visual spatial attention, whereas a sizeable ICA Component 3 was also observed in our Experiment 2, where visual spatial attention appears to be much less important than in the Experiment 1.

The functional significance of the different generator structures contributing to P300 as reported in the literature is relatively unclear. As one step towards a clarification of this issue, it was possible in the present experiments to attribute sequential effects in P300 amplitude to deep structures like subcortical regions or the cingulate cortex. This is in line with suggestions about the functions of these structures. Rogers et al. (1991) proposed that anterior thalamic structures are important for the initiation of the response, independent of the stimulus modality. In a similar vein Kropotov and Ponomarev (1991) suggested that their subcortical P300-like activity reflects a mechanism which selects a specific response from a set of possible programs. More specifically, Menon et al. (1997) pointed out that the anterior nucleus of the thalamus serves as a relay for the limbic system and receives inputs from the hippocampus via afferents from the hypothalamus. On the other hand, the anterior nucleus of the thalamus sends efferents to the cingulate cortex. Recently, the cingulate cortex has also been discussed as a potentially important systems for response selection processes (for a review, see Carter, Botvinick, & Cohen, 1999).

Together, our data consistently suggest the existence of separate neural generator contributions to P300. Superior-temporal and parietal generators appear to be responsible for the parietocentral subcomponent. These generators are not sensitive to the local sequence of successive events. A later contribution generates a subcomponent of P3 with a more anterior scalp distribution, possibly originating in mesial subcortical or cingulate structures. It is this subsystem that is affected by the sequence of preceding stimulus-response cycles and its function might be related to response-selection influencing processes. Furthermore this subcomponent is

overlapped by movement-related activity in the somatosensory cortex that also shows sequence sensitivity, explaining the "paradoxical" lateralization of sequential effects.

Conclusions

The present study replicated the finding of Sommer et al. (1999) that the cost-benefit pattern in P300 amplitude is very robust even when RT patterns change. Topographical analysis by means of ICA confirmed that the sequence-sensitive aspect of P300 can be separated from a more posterior portion of P300 that shows no sequential effects. This supports views of multiple dissociable subcomponents constituting the P300 complex. Furthermore it was found that the sequence-sensitive subcomponent shows a scalp topography dependent on the responding hand. A dipole source analysis suggests that the hand specificity of the sequence-sensitive ICA component results from overlap with somatosensory activity.

REFERENCES

Bell, A. J., & Sejnowski, T. J. (1995). An information maximization approach to blind separation and blind deconvolution. *Neural Computation*, *7*, 1129–1159.

Bell, A. J., & Sejnowski, T. J. (1996). Learning the higher-order structure of a natural sound. *Network: Computation in Neural Systems*, *7*, 261–270.

Bertelson, P. (1963). S-R relationships and reaction times to new versus repeated signals in a serial task. *Journal of Experimental Psychology*, *65*, 478–484.

Bertelson, P., & Renkin, A. (1966). Reaction times to new versus repeated signals in a serial task as a function of response-signal time interval. *Acta Psychologica*, *25*, 132–136.

Bötzel, K., Plendl, H., Paulus, W., & Scherg, M. (1993). Bereitschaftspotential: Is there a contribution of the supplementary motor area? *Electroencephalography and Clinical Neurophysiology*, *89*, 187–196.

Carter, C. S., Botvinick, M. M., & Cohen, J. D. (1999). The contribution of the anterior cingulate cortex to executive processes in cognition. *Reviews in the Neuroscience*, *10*, 49–57.

Coles, M. G. H. (1989). Modern mind-brain reading: Psychophysiology, physiology, and cognition. *Psychophysiology*, *26*, 251–269.

Cover, T. H., & Thomas, J. A. (1991). *Elements of information theory*. New York: John Wiley.

Dien, J. (1999). Differential lateralization of trait anxiety and trait fearfulness: Evoked potential correlates. *Personality and Individual Differences*, *26*, 333–356.

Donchin, E., & Coles, M. G. H. (1988). Is the P300 component a manifestation of context updating? *Behavioral and Brain Sciences*, *11*, 357–374.

Duncan-Johnson, C. C., & Donchin, E. (1977). On quantifying surprise: The variation of event-related potentials with subjective probability. *Psychophysiology*, *14*, 456–467.

Duncan-Johnson, C. C., Roth, W. T., & Kopell, B. S. (1984). Effects of stimulus sequence in P300 and reaction time in schizophrenics—a preliminary report. *Annals of the New York Academy of Sciences*, *425*, 570–577.

Ebmeier, K. P., Steele, J. D., MacKenzie, D. M., O'Carroll, R. E., Kydd, R. R., Glabus, M. F., Blackwood, D. H., Rugg, M. D., & Goodwin, G. M. (1995). Cognitive brain potentials and regional cerebral blood flow equivalents during two- and three-sound auditory "oddball tasks". *Electroencephalography and Clinical Neurophysiology*, *95*, 434–443.

Ford, J. M., Duncan-Johnson, C. C., Pfefferbaum, A., & Kopell, B. S. (1982). Expectancy for events in old age: Stimulus sequence effects on P300 and reaction time. *Journal of Gerontology*, *37*, 696–704.

Ghahremani, D., Makeig, S., Jung, T.-P., Bell, A. J., & Sejnowski, T. J. (1996). Independent Component Analysis of simulated EEG using a three-shell spherical head model, *Institute for Neural Computation Technical Report 96-01*, University of California San Diego, La Jolla, CA.

Gonsalvez, C. J., Gordon, E., Anderson, J., Pettigrew, G., Barry, R. J., Rennie, C., & Meares, R. (1995). Numbers of preceding nontargets differentially affect responses to targets in normal volunteers and patients with schizophrenia: A study of event-related potentials. *Psychiatry Research*, *58*, 69–75.

Halgren, E., Marinkovic, K., & Chauvel, P. (1998). Generators of the late cognitive potentials in auditory and visual oddball tasks. *Electroencephalography and Clinical Neurophysiology*, *106*, 156–64

Hyman, R. (1953). Stimulus information as a determinant of reaction time. *Journal of Experimental Psychology*, *45*, 188–196.

Johnson, R., Jr. (1986). A triarchic model of P300 amplitude. *Psychophysiology*, *23*, 367–384.

Johnson, R., Jr. (1988). The amplitude of the P300 component of event-related Potentials: Review and synthesis. In P. K. Ackles, J. R. Jennings, & M. G. H. Coles (Eds.), *Advances in Psychophysiology* (Vol. 3, pp. 69–138). Greenwich, London: JAI Press.

Johnson, R., Jr. (1993). On the neural generators of the P300 component of the event-related potential. *Psychophysiology*, *30*, 90–97.

Kirby, N. H. (1980). Sequential effects in choice reaction time. In A. T. Welford (Ed.), *Reaction times* (pp. 129–172). London: Academic Press.

Kok, A. (1988). Overlap between P300 and movement-related potentials: A response to Verleger. *Biological Psychology*, *27*, 51–58.

Kristeva-Feige, R., Rossi, S., Pizzella, V., Sabato, A., Tecchio, F., Feige, B., Romani, G. L., Edrich, J., & Rossini, P. M. (1996). Changes in movement-related brain activity during transient deafferentation: a neuromagnetic study. *Brain Research*, *714*, 201–208.

Kropotov, J. D., & Etlinger, S. C. (1999). Selection of actions in the basal ganglia-thalamocortical circuits: Review and model. *International Journal of Psychophysiology*, *31*, 197–217. Review.

Kropotov, J. D., & Ponomarev, V. A. (1991). Subcortical neuronal correlates of component P300 in man. *Electroencephalography and Clinical Neurophysiology*, *78*, 40–49.

Leuthold, H. & Jentzsch, I. (2001). Neural Correlates of Advance Movement Preparation: Dipole Source Analysis Approach. *Cognitive Brain Research*, in press.

Leuthold, H., & Sommer, W. (1993). Stimulus presentation rate dissociates sequential effects in event-related potentials and reaction time. *Psychophysiology*, *30*, 510–517.

Linden, D. E. G., Prvulovic, D., Formisano, E., Völlinger, M., Zanella, F. E., Goebel, R., & Dierks, T. (1999). The functional neuroanatomy of target detection: An fMRI study of visual and auditory oddball tasks. *Cerebral Cortex*, *9*, 815–823.

Linkser, R. (1992). Local synaptic learning rules suffice to maximize mutual information in a linear network. *Neural Computation*, *4*, 691–702.

Makeig, S., Jung, T.-P., Ghahremani, D., & Sejnowski, T. J. (1996). Independent Component Analysis of simulated ERP data. *Institute for Neural Computation Technical Report 96-06*, University of California San Diego, La Jolla, CA.

Makeig, S., Jung, T.-P., Bell, A. J., Ghahremani, D., & Sejnowski, T. J. (1997). Blind separation of auditory event-related brain responses into independent components. *Proceedings of the National Academy of Sciences of the USA* (MATLABTM code available on the web at HTTP://www.cnl.salk.edu/~scott).

Makeig, S., Westerfield, M., Jung, T.-P., Covington, J., Townsend, J., Sejnowski, T. J., & Courchesne, E. (1999). Functionally Independent Components of the late positive event-related potentials during visual spatial attention. *Journal of Neuroscience*, *19*, 2665–2680.

Matt, J., Leuthold, H., & Sommer, W. (1992). Differential effects of voluntary expectancies on reaction times and event-related potentials: Evidence for automatic and controlled expectancies. *Journal of Experimental Psychology: Learning, Memory, and Cognition*, *18*, 810–822.

McCarthy, G., Luby, M., Gore, J., & Goldman-Rakic, P. (1997). Infrequent events transiently activate human prefrontal and parietal cortex as measured by functional MRI. *Journal of Neurophysiology*, *77*, 1630–1634.

Mecklinger, A., Maess, B., Opitz, B., Pfeifer, E., Cheyne, D., & Weinberg, H. (1998). A MEG analysis of the P300 in visual discrimination tasks. *Electroencephalography and Clinical Neurophysiology*, *108*, 45–56.

Mecklinger, A., & Ullsperger, P. (1995). The P300 to novel and target events: A spatiotemporal dipole model analysis. *Neuroreport*, *7*, 241–245.

Menon, V., Ford, J. M., Lim, K. O., Glover, G. H., & Pfefferbaum, A. (1997). Combined event-related fMRI and EEG evidence for temporal-parietal cortex activation during target detection. *Neuroreport*, *8*, 3029–3037.

Miller, J., Riehle, A., & Requin, J. (1992). Effects of preliminary perceptual

output on neuronal activity of the primary motor cortex. *Journal of Experimental Psychology: Human Perception and Performance*, *18*, 1121–1138.
Nadal, J.-P., & Parga, N. (1994). Non-linear neurons in the low noise limit: A factorial code maximizes information transfer. *Network*, *5*, 565–581.
Oldfield, R. C. (1971). The assessment and analysis of handedness: The Edinburgh Investory. *Neuropsychologia*, *9*, 97–113.
Opitz, B., Mecklinger, A., von Cramon, D. Y., & Kruggel, F. (1999). Combining electrophysiological and hemodynamic measures of the auditory oddball. *Psychophysiology*, *36*, 142–147.
Praamstra, P., Stegemann, D. F., Horstink, M. W. I. M., & Cools, A. R. (1996). Dipole source analysis suggests selective modulation of the supplementary motor area contribution to the readiness potential. *Electroencephalography and Clinical Neurophysiology*, *98*, 468–477.
Roberts, L. E., Rau, H., Lutzenberger, W., & Birbaumer, N. (1994). Mapping P300 waves onto inhibition: Go/No-Go discrimination. *Electroencephalography and Clinical Neurophysiology*, *92*, 44–55.
Rogers, R. L., Baumann, S. B., Papanicolaou, A. C., Bourbon, T. W., Alagarsamy, S., & Eisenberg, H. M. (1991). Localization of the P3 sources using magnetoencephalography and magnetic resonance imaging. *Electroencephalography and Clinical Neurophysiology*, *79*, 308–321.
Scherg, M., & Berg, P. (1996). *BESA Version 2.2 Handbook*. Munich: Megis.
Soetens, E., Boer, L. C., & Hueting, J. E. (1985). Expectancy or automatic facilitation? Separating sequential effects in two-choice reaction time. *Journal of Experimental Psychology: Human Perception and Performance*, *11*, 598–616.
Soetens, E., Deboeck, M., & Hueting, J. (1984). Automatic aftereffects in two-choice Reaction time: A mathematical representation of some concepts. *Journal of Experimental Psychology: Human Perception and Performance*, *10*, 581–598.
Sommer, W., Leuthold, H., & Matt, J. (1998). The expectancies that govern the P300 amplitude are mostly automatic and unconscious. *Behavioral and Brain Sciences*, *21*, 149–150.
Sommer, W., Leuthold, H., & Soetens, E. (1999). Covert signs of expectancy in serial reaction time tasks revealed by event-related potentials. *Perception & Psychophysics*, *61*, 342–352.
Sommer, W., Matt, J., & Leuthold, H. (1990). Consciousness of attention and expectancy as reflected in event-related potentials and reaction times. *Journal of Experimental Psychology: Learning, Memory, and Cognition*, *16*, 902–915.
Spencer, K. M., Dien, J., & Donchin, E. (1999). A componential analysis of the ERP elicited by novel events using a dense electrode array. *Psychophysiology*, *36*, 409–414.
Squires, K. C., Wickens, C. D., Squires, N. K., & Donchin, E. (1976). The effect of stimulus sequence on the waveform of the cortical event-related potential. *Science*, *193*, 1142–1146.
Tarkka, I. M., & Stokic, D. S. (1998). Source localization of P300 from oddball, single stimulus, and omitted-stimulus paradigms. *Brain Topography*, *11*, 141–151.
Tarkka, I. M., Stokic, D. S., Basile, L. F., & Papanicolaou, A. C. (1995). Electric source location of the P300 agrees with magnetic source location. *Electroencephalography and Clinical Neurophysiology*, *96*, 538–545.
Tucker, D. M., Liotti, M., Potts, G. F., Russell, G. S., & Posner, M. I. (1994). Spatiotemporal analysis of brain electrical fields. *Human Brain Mapping*, *1*, 134–152.
Verleger, R. (1988). Event-related potentials and cognition: A critique of the context updating hypothesis and an alternative interpretation of P3. *Behavioral and Brain Sciences*, *11*, 343–356.
Weinrich, M., Wise, S. P., & Mauritz, K. H. (1984). A neurophysiological study of the premotor cortex in rhesus monkey. *Brain*, *107*, 385–414.
Woldorff, M. G. (1993). Distortion of ERP averages due to overlap from temporally adjacent ERPs: Analysis and correction. *Psychophysiology*, *30*, 98–119.
Yordanova, J., Devrim, M., Kolev, V., Ademoglu, A., & Demiralp, T. (2000). Multiple time-frequency components account for the complex functional reactivity of P300. *Neuroreport*, *7*, 1097–1103.
Yoshiura, T., Zhong, J., Shibata, D. K., Kwok, W. E., Shrier, D. A., & Numaguchi, Y. (1999). Functional MRI study of auditory and visual oddball tasks. *Neuroreport*, *10*, 1683–1688.

(Received April 25, 2000; Accepted December 6, 2000)

APPENDIX

To derive the dipole source model for the movement-related activity we used a strategy described in Praamstra, Stegemann, Horstink, and Cools (1996) and Leuthold and Jentzsch (2001). In the following the procedure is described in more detail.

To derive a dipole source model of movement-related activity, two steps are required previous to modeling. First, it is necessary to calculate ERP epochs that are time locked to the response. To do this, the continuous EEG record was separated into 1,000-ms epochs, starting 600 ms before response onset, resulting in response-synchronized ERPs. Second, all movement-unrelated activity was removed from the ERP data by calculating the lateralized ERP activity (L-ERP) as follows. For each trial, the ERPs over the

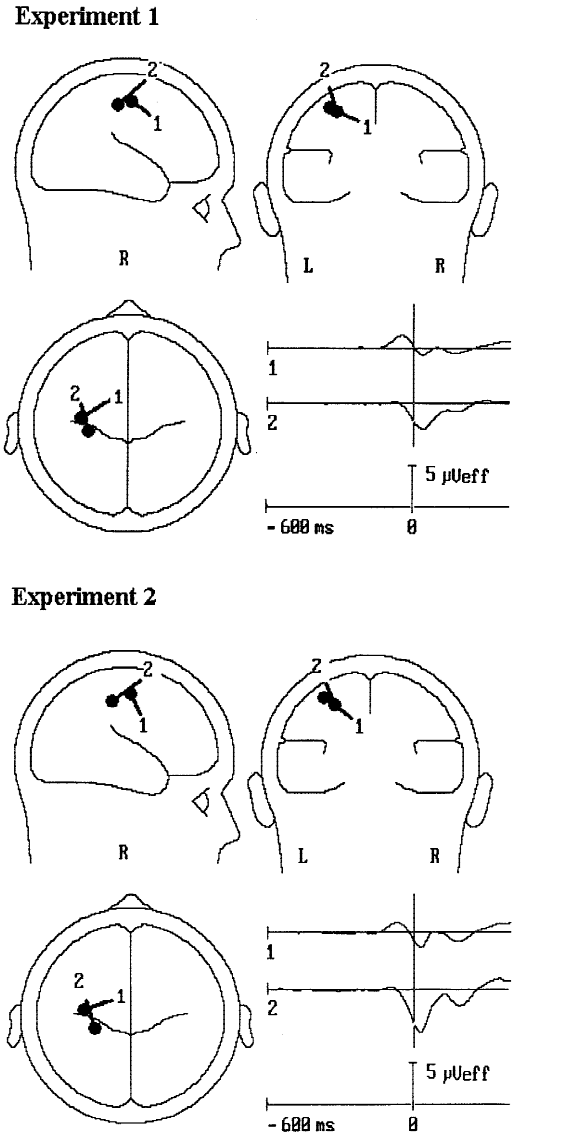

Figure 12. Dipole source models and corresponding source waveforms of the isolated lateralized movement-related activity (L-ERP) for Experiment 1 (left) and Experiment 2 (right). Note, that the figure represents only half the model, as, for ease of visualization, the antisymmetrical sources in the other hemisphere are omitted.

electrodes ipsilateral to the demanded-response hand were subtracted from the ERPs at corresponding contralateral electrodes sites. To eliminate all hand-independent asymmetries in the next step left-hand and right-hand difference waves were averaged, yielding the L-ERP.

Dipole modeling of lateralized movement-related activity was done by using antisymmetrically projected L-ERP data. That is, L-ERPs were projected to one hemisphere and copied to the other hemisphere with polarities inverted (Praamstra et al., 1996). Perimovement activity was modeled during a 200-ms interval beginning 150 ms before response onset. The minimal number of dipoles that should be included into the model was estimated by spatial PCA. In both experiments, two principal components were sufficient to explain 99% of the data variance. In Experiment 1, the two components explained 80.5% and 19.4% of the data variance, respectively. In Experiment 2 they explained 71.3% and 28.5%, respectively. A dipole model for the L-ERP distribution was obtained by using a sequential fitting strategy (cf. Scherg & Berg, 1996), because in the interval −150 to −50 ms prior to response onset just one PCA component explained all data variance (Experiment 1: 99.8%; Experiment 2: 98.7%). Therefore, a first antisymmetric dipole pair was fitted in this interval and accounted for nearly all the variance in both experiments (Experiment 1: RV = 0.3%; Experiment 2: RV = 2.9%). When the upper limit of the fit interval was increased, RV started to increase rapidly, suggesting the growing influence of a second source. Therefore, a second pair of dipoles was fitted in the time interval from −150 ms to +50 ms with the first pair of dipoles held fixed. The resulting dipole model accounted for 99.3% (Experiment 1) and 97.8% (Experiment 2) of the variance in this 200-ms time interval. The source starting first was located more anteriorly as compared to the source starting subsequently, possibly reflecting primary motor cortex (MI) activity, whereas the second source might originate from reafferent activity in somatosensory areas (Bötzel, Plendl, Paulus, & Scherg, 1993; Kristeva-Feige et al., 1996). The models for both experiments are shown in Figure 12.